phosphorylated extracellular signal-regulated kinase (ERK) via inhibiting phosphatase binding to ERK.[34] We performed Western Blot analysis to show if SU1498 cause accumulation of phosphorylated ERK in mESCMs. Phosphorylation of ERK was increased only when cells were treated by SU1498 but not with BIO or KN93 (Figure 3b). Then we determined whether SU1498-elicited mESCM proliferation is mediated by ERK signaling. Treatment with a MAPK/ERK kinase (MEK) inhibitor PD98059 (PD) that inhibits ERK phosphorylation abolished the increase in SU1498-induced mESCMs (Figure 3c). In addition, ZM336372 (ZM), an activator of Raf1/ERK signaling, similarly increased mESCM number (Figure 3c). Furthermore, an ERK activating growth factor, NRG1β, also increased mESCM numbers by approximately 1.5 times (data not shown) as reported.[9,35] Taken together, these data indicate that SU1498 increase cardiomyocyte proliferation through activation of Raf-MEK-ERK signal cascade.[7,36]

CaMKII was reported to be involved in cardiomyocyte hypertrophy, but little is known about its role in cardiomyocyte proliferation. Two distinct CaMKII inhibitors, KN93 and KN62, similarly increased cardiomyocyte numbers (Figure 3d), suggesting that CaMKII is a novel regulator of cardiomyocyte proliferation. We investigated the role of CaMKII in cardiomyocyte proliferation. CaMKII is a family protein coded by the *Camk2a*, *Camk2b*, *Camk2d* and *Camk2g* isoform genes. Among them, *Camk2a*, *Camk2d* and *Camk2g* mRNA but not *Camk2b* mRNA expressions were detected in purified mESCM at Flkd6 (data not shown). We evaluated the effect of specific small interfering RNA (siRNA) against each CaMKII isoform to identify the main isoform(s) that inhibit mESCM proliferation. Specific knockdown of *Camk2d* and *2g*, the major CaMKII isoforms in cardiomyocytes[37], by siRNA increased mESCM cell numbers by 50% (Figure S3a–b). Conversely, knockdown of *Camk2a* reciprocally decreased mESCM numbers (Figure S3b). These data suggest that KN93 and KN62 increase mESCM by inhibiting CaMKIId/g. Knockdown of *Camk2d* but not *Camk2g* by siRNA resulted in 50% reduction of *Ink4b* expression similar to KN93 treatment (Figure S3c). Furthermore, reduction of *Ink4b* with siRNA significantly increased mESCM numbers (Figure S3d–e). These data suggest that CaMKIId negatively regulates mESCM proliferation through Ink4b.

Our results, thus, show that these chemicals affect cardiomyocyte proliferation through distinct pathways–BIO/GSK3, SU1498/ERK, and KNs/CaMKII.

Combinatory Effects of Chemicals on mESCM Proliferation

Distinct molecular targets of these chemicals prompted us to examine combinations of inhibitors to maximize their proliferative effects. We first examined combinations of two inhibitors. BIO+SU1498 (SU) and BIO+KN93 (KN) significantly increased mESCM proliferation (Figure 4a). Unexpectedly, a combination of SU+KN cancelled their individual effects. Additionally a combination of all three inhibitors, BIO+SU+KN, neither showed any effect on cardiomyocyte proliferation (Figure 4a), suggesting that SU1498 and KN93 could be conflicting in the cardiomyocyte proliferation machinery. A p38 MAPK inhibitor SB203580 (p38i) is known to increase neonatal or adult cardiomyocyte proliferation.[38] In fact, p38i (1 μM) significantly increased the mESCM number by approximately twofold also in our experimental system (Figure 4b). Therefore, we added p38i to each combination, and found that BIO+SU+p38i and BIO+KN+p38i increased in mESCM numbers up to 6–7 times more than control until the mESCMs reached confluency (data not shown). To allow more robust proliferation, we next tested mESCM culture at a lower cell density (5.0×10^4 / well (6-well plate)). In this condition, the BIO+SU+p38i combination increased mESCM up to 14-fold (Figure 4c). We also examined cell cycle of mESCMs treated with each combination (Figure 4d). Both combinations (BIO+SU+p38i and BIO+KN+p38i) significantly increased EdU (3hr pulse) incorporation to approximately 2.5 and 4 times more than DMSO treatment

at Flkd6+3 and Flkd6+5, respectively (Figure 4d). These combinations also significantly increased pH3 in mESCMs up to approximately 2.7 and 2.5 times more than DMSO treatment at Flkd6+3 and Flkd6+5, respectively (Figure 4d). We also evaluated 4N fraction (G2/M and binucleated cardiomyocytes) by flow cytometry, but there were no significant differences (data not shown). Thus, we successfully demonstrated that optimal combinations of the chemicals effectively induced substantial cardiomyocyte proliferation. We, collectively, named these seven chemicals (BIO, CHIR99021, SU1498, ZM336372, KN93, KN62 and p38i) as cardiomyocyte proliferative chemicals (CPCs).

We further confirmed cardiomyocyte features after proliferation. All αMHC-EGFP-positive cells used in our study were also positive for cTnT (Figure S1). These cells were spontaneously beating before and after the chemical treatments. Proliferated cardiomyocytes with combined CPC treatments (BIO+SU1498+p38i and BIO+KN93+p38i) showed similar cardiomyocyte-like action potentials (Figure S4a). The main parameters of action potentials, maximum diastolic potential (MDP), maximum rate of rise of the action potential (dv/dt) and action potential duration (ADP50), were not different among control and CPC-treated mESCMs (Figure S4b). Cardiac myosins (*Myh6*, *Myh7*, *Myl2* and *Myl7*), mature cardiac markers, were increased more than two-eight times during robust proliferation with combined CPCs (BIO+SU1498/KN93+p38i) from Flkd6 to Flkd6+5 (Figure S4c). The data demonstrated that CPCs enhanced proliferation of cardiomyocytes with no apparent bias in cardiomyocyte features.

Developmental Stage Specific Effects of Chemicals on Embryonic, Neonatal and Adult Cardiomyocytes

Next, we examined the effects of CPCs on cardiomyocytes in various developmental stages, such as embryos, neonates and adults.

Cardiomyocytes isolated from the hearts of E9.5 mice, which is in comparable differentiation stage to mESCMs[39], were cultured and treated with each CPC or with the combinations for 3–5 days (E9.5+3 and E9.5+5, respectively). Each CPC treatment increased the S phases and M phases in embryonic cardiomyocytes at E9.5+3 (Figure S5a). Combined CPC treatments (BIO+p38i+SU/KN) increased S phase to approximately 4.5 times and M phase to 3 times more than control at E9.5+3 (Figure S5a). Combined CPC treatments rapidly increased embryonic cardiomyocyte nuclei number up to 8.5 times more than control at E9.5+5 (Figure S5). These data indicated that CPCs efficiently proliferate embryonic cardiomyocytes in a similar manner to those in mESCMs.

Neonatal (P3) rat ventricular cardiomyocytes (NRVCs) were isolated and cultured with CPCs for 2 days. As a baseline, DMSO-treated neonatal cardiomyocytes rarely proliferated (BrdU-positive cells, 3.4±0.3%; pH3-positive cells, 0.37±0.08%; Aurora B-positive cells, 0.36±0.04%). BIO, SU1498 or p38i alone increased in number of BrdU-positive cardiomyocytes by 2–3.5 times (Figure 5a). In contrast to mESCMs and embryonic cardiomyocytes, KN93 failed to increase BrdU incorporation and further progression of the cell cycle in NRVCs (BrdU-positive cells, 4.1±1.4%, Figure 5a). Combination of BIO+p38i synergistically increased BrdU incorporation and BIO+SU+p38i further enhanced the BrdU incorporation (19.4±2.2% and 25.0±2.6%, respectively. $p < 0.05$ *vs.* control. Figure 5a). In BIO+p38i and BIO+p38i+SU1498 condition, the cell cycle progression to M phase (pH3-positive, 3.70±0.20% and 4.03±0.19%, respectively. Figure 5b) and cell division (Aurora B-positive, 3.47±0.21% and 3.76±0.24%, respectively. Figure 5c) were significantly increased compared to the baseline.

Adult rat cardiomyocytes were isolated and cultured with CPCs for 6 days. Less than 0.01% of adult cardiomyocytes were positive for BrdU and none of them were pH3-positive at the

baseline (DMSO treatment). BIO or p38i treatment alone evoked cell cycle reentry in adult cardiomyocytes, that is, BrdU-positive and pH3-positive cells were increased (Figure 5d). Combination of BIO and p38i synergistically and significantly enhanced the cell cycle progression markers in adult cardiomyocytes compared to baseline (BrdU-positive cells, 2.7±0.3%; pH3-positive cells, 0.60±0.05%; Aurora B-positive cells, 0.37±0.07%) (Figure 5d–g). pH3-positive metaphase and anaphase cardiomyocytes were found in BIO+p38i condition (Figure 5f). In contrast, SU1498 and KN93 failed to enhance the effects of BIO +p38i (Figure 5d and e).

These findings suggest that GSK3 and p38 MAPK are broadly and cooperatively regulating various cardiomyocytes including in adults whereas ERK and CaMKII play a novel developmental stage-specific function.

Effects of Chemicals on Cardiomyocytes from Human iPSCs and ESCs

Finally, we evaluated the effects of CPCs on human iPSC- and ESC-derived cardiomyocytes. A human iPSC line 201B6 is one of the most characterized four-factor (Oct3/4, Sox2, c-myc and Klf4)-iPSCs for differentiation properties, including cardiac differentiation.[28,40] Cardiomyocytes (hiPSCMs) were induced with a two-dimensional, defined, serum-free condition-based cardiomyocyte differentiation method (Figure 6a).[22,28] Spontaneously-beating hiPSCMs appeared around d8–10 after Activin A treatment. At day 11, CPC treatment was started. The cell cycle was evaluated by flow cytometry at day 14, and the cardiomyocyte number was calculated at day 16. In agreement with the results from mESCMs, BIO+p38i+SU significantly increased EdU incorporation in hiPSCMs at d14 (Figure 6b–c) and hiPSCM number at d16 (Figure 6d). BIO+p38i+KN had tendencies to increase EdU incorporation and hiPSCM number (Figure 6b–d). Similarly, BIO+p38i+SU increased BrdU incorporation in hESC-derived cardiomyocytes by approximately 1.5 times (data not shown). We purified hiPSCMs with a recently identified cell-surface marker for hiPSCMs, VCAM1[28], and evaluated structural and functional features of CPC-expanded hiPSCMs. CPC-expanded hiPSCMs showed clear sarcomere formation (Figure 6e) and action potentials (Figure 6f), similar to those in control hiPSCMs. These data indicate that CPCs also successfully work in human cardiomyocytes.

Discussion

In the present study, we screened a chemical library with a HCS for effects on the proliferation of mESCMs and succeeded in identifying several distinct chemicals promoting cardiomyocyte proliferation. These findings uncovered common and developmental stage-specific machineries controlling cardiomyocyte proliferation. They also would provide broad and efficient ways of manipulating cardiomyocyte number from embryos to adults and in mouse and human.

We identified chemicals regulating four distinct signaling pathways, namely GSK3 (BIO and CHIR99021), ERK (SU1498 and ZM336372), CaMKII (KN93 and KN62) and p38 MAPK (SB203580) (Fig. 7). Consistent with previous reports[32,38], GSK3 and p38 MAPK signal cascades negatively regulated cardiomyocyte proliferation and inhibitors of these kinases enhanced rodent and human cardiomyocyte proliferation. This is the first report to show synergistic effects of combinatorial inhibition of GSK3 and p38 MAPK, especially on adult cardiomyocyte proliferation.

In contrast to GSK3 and p38 MAPK inhibitors, ERK activators and CaMKII inhibitors have not been reported to be involved in cardiomyocyte proliferation. Raf-MEK-ERK signal cascade positively regulates the proliferation of cardiomyocytes as a downstream target of growth factors.[7,8] Furthermore, phospho-ERK is evident in E8.0 heart, which depends on

the FGF receptor.[41] SU1498 enhances ERK phosphorylation through inhibiting phosphatase (Figure 3b).[34] Phosphatases, such as dual-specificity phosphatase 6 (Dusp6), negatively regulate ERK phosphorylation.[42] Dusp6 null mice showed enhanced ERK phosphorylation and increased cardiomyocyte proliferation during embryonic development and in the early postnatal period.[36] Dusp6 is a possible candidate for a SU1498 target. A Raf activator, ZM336372, also showed a similar pro-proliferative effect. Collectively, all of these results indicate that activation of Raf-MEK-ERK pathway could be a potent molecular target to induce cardiomyocyte proliferation. CaMKII has been reported to regulate cardiac hypertrophy in the later stages of development or in adults.[43,44] Here we showed that in an earlier developmental stage corresponding to E9.5 mouse embryos, CaMKII could inhibit cardiomyocyte proliferation. We confirmed phosphorylation of CaMKII in early mouse embryos (E9.5 and E13.5) and found that CaMKII phosphorylation was drastically increased between E9.5 and E13.5 (Figure S6). CaMKII phosphorylation was more evident in trabecular layer cardiomyocytes than in compact layer counterparts at E13.5. This timing of CaMKII activation in trabecular cardiomyocytes is in accordance with the period when the proliferative ability of trabecular layer cardiomyocytes is reduced[13], suggesting that CaMKII at this differentiation stage could be involved in growth arrest of early cardiomyocytes. CaMKII inhibitors lost its proliferative effect on postnatal and adult cardiomyocytes, suggesting that the growth inhibitory effect of CaMKII has an early developmental stage-specific effect, and switching of its effect to hypertrophy would occur in the later stage. Currently, the precise molecular mechanisms for the developmental stage-specific CaMKII effect are unknown, but this finding is a clue to the precise understanding of CaMKII functions in cardiomyocytes.

Though ERK activators and CaMKII inhibitors did not show sufficient proliferative effects in adult cardiomyocytes, our finding of an effective chemical cocktail for cardiomyocyte proliferation can offer a therapeutic potential for cardiac regeneration. In diseased hearts, cardiomyocytes express embryonic genes[45], and small fraction of cardiomyocytes is de-differentiated and proliferating[3] or newly differentiated from progenitor cells[46], indicating that these cardiomyocytes in diseased hearts are in a more immature stage. Hence, not only will the combination of GSK inhibitors and p38i but also our effective cocktails including three chemicals exert their potent pro-proliferative effects in diseased hearts, facilitating cardiac regeneration.

Recently, PSC-derived cells have drawn considerable interest for use in drug screening, disease modeling[20,21,47] and for regenerative medicine as cell therapies[48] are highlighted. In addition, PSC-derived cells can provide an experimental system for studying cellular physiology especially in cell types difficult to obtain from adults. With the use of our PSC systems, it is likely that other more effective chemicals would be identified from other libraries. Thus, our novel screening system for cardiomyocyte proliferation combining stem cell technology and chemical biology could be a potent tool for investigating efficient molecules and largely contribute to future cardiac regenerative medicine, especially through regeneration with drugs.

Supplementary Material

Refer to Web version on PubMed Central for supplementary material.

Acknowledgments

We thank Prof. Shinya Yamanaka for the generous gift of human iPS cells (201B6). We thank the Screening Committee of Anticancer Drugs supported by Grant-in-Aid for Scientific Research on Priority Area 'Cancer' from The Ministry of Education, Culture, Sports, Science and Technology for the generous gift of The SCADS inhibitor

kit. We also thank Mr. Yukihiro Furuyama (Molecular Devices Japan, Tokyo, Japan) for technical assistant for high content imaging, and Drs. Meiko Takahashi and Mark Ranek for critical reading of the manuscript.

Funding Sources: This work was supported by grants from the Ministry of Education, Science, Sports and Culture of Japan, the Ministry of Health, Labour and Welfare, the Project for Realization of Regenerative Medicine, and Japan Science and Technology Agency. H.U. and H.F. are supported by the Japan Society for the Promotion of Science.

References

1. Bergmann O, Bhardwaj RD, Bernard S, Zdunek S, Barnabé-Heider F, Walsh S, et al. Evidence for cardiomyocyte renewal in humans. Science. 2009; 324:98–102. [PubMed: 19342590]
2. Kajstura J, Gurusamy N, Ogórek B, Goichberg P, Clavo-Rondon C, Hosoda T, et al. Myocyte turnover in the aging human heart. Circ Res. 2010; 107:1374–1386. [PubMed: 21088285]
3. Senyo SE, Steinhauser ML, Pizzimenti CL, Yang VK, Cai L, Wang M, et al. Mammalian heart renewal by pre-existing cardiomyocytes. Nature. 2013; 493:433–436. [PubMed: 23222518]
4. Bicknell KA, Coxon CH, Brooks G. Can the cardiomyocyte cell cycle be reprogrammed? J Mol Cell Cardiol. 2007; 42:706–721. [PubMed: 17362983]
5. Engel FB, Hsieh PCH, Lee RT, Keating MT. FGF1/p38 MAP kinase inhibitor therapy induces cardiomyocyte mitosis, reduces scarring, and rescues function after myocardial infarction. Proc Natl Acad Sci USA. 2006; 103:15546–15551. [PubMed: 17032753]
6. Shimoji K, Yuasa S, Onizuka T, Hattori F, Tanaka T, Hara M, et al. G-csf promotes the proliferation of developing cardiomyocytes in vivo and in derivation from escs and ipscs. Cell Stem Cell. 2010; 6:227–237. [PubMed: 20207226]
7. Ieda M, Tsuchihashi T, Ivey KN, Ross RS, Hong TT, Shaw RM, et al. Cardiac fibroblasts regulate myocardial proliferation through beta1 integrin signaling. Dev Cell. 2009; 16:233–244. [PubMed: 19217425]
8. Kühn B, del Monte F, Hajjar RJ, Chang YS, Lebeche D, Arab S, et al. Periostin induces proliferation of differentiated cardiomyocytes and promotes cardiac repair. Nat Med. 2007; 13:962–969. [PubMed: 17632525]
9. Bersell K, Arab S, Haring B, Kühn B. Neuregulin1/erbb4 signaling induces cardiomyocyte proliferation and repair of heart injury. Cell. 2009; 138:257–270. [PubMed: 19632177]
10. Singh MK, Li Y, Cobb RM, Zhou D, Lu MM, Epstein JA, et al. Gata4 and gata5 cooperatively regulate cardiac myocyte proliferation in mice. J Biol Chem. 2010; 285:1765–1772. [PubMed: 19889636]
11. Trivedi CM, Lu MM, Wang Q, Epstein JA. Transgenic overexpression of hdac3 in the heart produces increased postnatal cardiac myocyte proliferation but does not induce hypertrophy. J Biol Chem. 2008; 283:26484–26489. [PubMed: 18625706]
12. Campa VM, Gutiérrez-Lanza R, Cerignoli F, Díaz-Trelles R, Nelson B, Tsuji T, et al. Notch activates cell cycle reentry and progression in quiescent cardiomyocytes. J Cell Biol. 2008; 183:129–141. [PubMed: 18838555]
13. Toyoda M, Shirato H, Nakajima K, Kojima M, Takahashi M, Kubota M, et al. Jumonji downregulates cardiac cell proliferation by repressing cyclin d1 expression. Dev Cell. 2003; 5:85–97. [PubMed: 12852854]
14. Mahmoud AI, Kocabas F, Muralidhar SA, Kimura W, Koura AS, Thet S, et al. Meis1 regulates postnatal cardiomyocyte cell cycle arrest. Nature. 2013; 497:249–253. [PubMed: 23594737]
15. Eulalio A, Mano M, Dal Ferro M, Zentilin L, Sinagra G, Zacchigna S, et al. Functional screening identifies miRNAs inducing cardiac regeneration. Nature. 2012; 492:376–381. [PubMed: 23222520]
16. Xu Y, Shi Y, Ding S. A chemical approach to stem-cell biology and regenerative medicine. Nature. 2008; 453:338–344. [PubMed: 18480815]
17. Nakao Y, Narazaki G, Hoshino T, Maeda S, Yoshida M, Maejima H, et al. Evaluation of antiangiogenic activity of azumamides by the in vitro vascular organization model using mouse induced pluripotent stem (ips) cells. Bioorg Med Chem Lett. 2008; 18:2982–2984. [PubMed: 18397826]

18. Zanella F, Lorens JB, Link W. High content screening: Seeing is believing. Trends Biotechnol. 2010; 28:237–245. [PubMed: 20346526]
19. Yoshida Y, Yamanaka S. Recent stem cell advances: Induced pluripotent stem cells for disease modeling and stem cell-based regeneration. Circulation. 2010; 122:80–87. [PubMed: 20606130]
20. Egawa N, Kitaoka S, Tsukita K, Naitoh M, Takahashi K, Yamamoto T, et al. Drug screening for ALS using patient-specific induced pluripotent stem cells. Sci Transl Med. 2012; 4:145ra104.
21. Kondo T, Asai M, Tsukita K, Kutoku Y, Ohsawa Y, Sunada Y, et al. Modeling Alzheimer's disease with iPSCs reveals stress phenotypes associated with intracellular Aβ and differential drug responsiveness. Cell Stem Cell. 2013; 12:487–496. [PubMed: 23434393]
22. Laflamme MA, Chen KY, Naumova AV, Muskheli V, Fugate JA, Dupras SK, et al. Cardiomyocytes derived from human embryonic stem cells in pro-survival factors enhance function of infarcted rat hearts. Nat Biotechnol. 2007; 25:1015–1024. [PubMed: 17721512]
23. Yamashita JK. Es and ips cell research for cardiovascular regeneration. Experimental cell research. 2010; 316:2555–2559. [PubMed: 20385126]
24. Yamashita J, Itoh H, Hirashima M, Ogawa M, Nishikawa S, Yurugi T, et al. Flk1-positive cells derived from embryonic stem cells serve as vascular progenitors. Nature. 2000; 408:92–96. [PubMed: 11081514]
25. Yamashita JK, Takano M, Hiraoka-Kanie M, Shimazu C, Peishi Y, Yanagi K, et al. Prospective identification of cardiac progenitors by a novel single cell-based cardiomyocyte induction. FASEB J. 2005; 19:1534–1536. [PubMed: 16033809]
26. Narazaki G, Uosaki H, Teranishi M, Okita K, Kim B, Matsuoka S, et al. Directed and systematic differentiation of cardiovascular cells from mouse induced pluripotent stem cells. Circulation. 2008; 118:498–506. [PubMed: 18625891]
27. Yan P, Nagasawa A, Uosaki H, Sugimoto A, Yamamizu K, Teranishi M, et al. Cyclosporin-A potently induces highly cardiogenic progenitors from embryonic stem cells. Biochem Biophys Res Commun. 2009; 379:115–120. [PubMed: 19094963]
28. Uosaki H, Fukushima H, Takeuchi A, Matsuoka S, Nakatsuji N, Yamanaka S, et al. Efficient and Scalable Purification of Cardiomyocytes from Human Embryonic and Induced Pluripotent Stem Cells by VCAM1 Surface Expression. PLoS ONE. 2011; 6:e23657. [PubMed: 21876760]
29. Kawada M, Inoue H, Masuda T, Ikeda D. Insulin-like growth factor i secreted from prostate stromal cells mediates tumor-stromal cell interactions of prostate cancer. Cancer Res. 2006; 66:4419–4425. [PubMed: 16618768]
30. Tsuchiya A, Tashiro E, Yoshida M, Imoto M. Involvement of protein phosphatase 2a nuclear accumulation and subsequent inactivation of activator protein-1 in leptomycin b-inhibited cyclin d1 expression. Oncogene. 2007; 26:1522–1532. [PubMed: 16964287]
31. Liu Z, Yue S, Chen X, Kubin T, Braun T. Regulation of cardiomyocyte polyploidy and multinucleation by cycling1. Circ Res. 2010; 106:1498–1506. [PubMed: 20360255]
32. Tseng AS, Engel FB, Keating MT. The gsk-3 inhibitor bio promotes proliferation in mammalian cardiomyocytes. Chem Biol. 2006; 13:957–963. [PubMed: 16984885]
33. Strawn LM, McMahon G, App H, Schreck R, Kuchler WR, Longhi MP, et al. Flk-1 as a target for tumor growth inhibition. Cancer Res. 1996; 56:3540–3545. [PubMed: 8758924]
34. Boguslawski G, McGlynn PW, Harvey KA, Kovala AT. Su1498, an inhibitor of vascular endothelial growth factor receptor 2, causes accumulation of phosphorylated erk kinases and inhibits their activity in vivo and in vitro. J Biol Chem. 2004; 279:5716–5724. [PubMed: 14625306]
35. Zhu WZ, Xie Y, Moyes KW, Gold JD, Askari B, Laflamme MA. Neuregulin/erbb signaling regulates cardiac subtype specification in differentiating human embryonic stem cells. Circ Res. 2010; 107:776–786. [PubMed: 20671236]
36. Maillet M, Purcell NH, Sargent MA, York A, Bueno OF, Molkentin JD. Dusp6 (mkp3) null mice show enhanced erk1/2 phosphorylation at baseline and increased myocyte proliferation in the heart affecting disease susceptibility. J Biol Chem. 2008; 283:31246–31255. [PubMed: 18753132]
37. Tobimatsu T, Fujisawa H. Tissue-specific expression of four types of rat calmodulin-dependent protein kinase ii mrnas. J Biol Chem. 1989; 264:17907–17912. [PubMed: 2553697]

38. Engel FB, Schebesta M, Duong MT, Lu G, Ren S, Madwed JB, et al. P38 map kinase inhibition enables proliferation of adult mammalian cardiomyocytes. Genes Dev. 2005; 19:1175–1187. [PubMed: 15870258]
39. Yanagi K, Takano M, Narazaki G, Uosaki H, Hoshino T, Ishii T, et al. Hyperpolarization-activated cyclic nucleotide-gated channels and T-type calcium channels confer automaticity of embryonic stem cell-derived cardiomyocytes. Stem Cells. 2007; 25:2712–2719. [PubMed: 17656646]
40. Takahashi K, Tanabe K, Ohnuki M, Narita M, Ichisaka T, Tomoda K, et al. Induction of pluripotent stem cells from adult human fibroblasts by defined factors. Cell. 2007; 131:861–872. [PubMed: 18035408]
41. Corson LB, Yamanaka Y, Lai KM, Rossant J. Spatial and temporal patterns of erk signaling during mouse embryogenesis. Development. 2003; 130:4527–4537. [PubMed: 12925581]
42. Jeffrey KL, Camps M, Rommel C, Mackay CR. Targeting dual-specificity phosphatases: Manipulating map kinase signalling and immune responses. Nat Rev Drug discov. 2007; 6:391–403. [PubMed: 17473844]
43. Zhu W, Zou Y, Shiojima I, Kudoh S, Aikawa R, Hayashi D, et al. Ca2+/calmodulin-dependent kinase ii and calcineurin play critical roles in endothelin-1-induced cardiomyocyte hypertrophy. J Biol Chem. 2000; 275:15239–15245. [PubMed: 10809760]
44. Backs J, Backs T, Neef S, Kreusser MM, Lehmann LH, Patrick DM, et al. The delta isoform of cam kinase ii is required for pathological cardiac hypertrophy and remodeling after pressure overload. Proc Natl Acad Sci USA. 2009; 106:2342–2347. [PubMed: 19179290]
45. Kuwahara K, Nishikimi T, Nakao K. Transcriptional regulation of the fetal cardiac gene program. J Pharmacol Sci. 2012; 119:198–203. [PubMed: 22786561]
46. Hsieh PCH, Segers VFM, Davis ME, MacGillivray C, Gannon J, Molkentin JD, et al. Evidence from a genetic fate-mapping study that stem cells refresh adult mammalian cardiomyocytes after injury. Nat Med. 2007; 13:970–974. [PubMed: 17660827]
47. Moretti A, Bellin M, Welling A, Jung CB, Lam JT, Bott-Flügel L, et al. Patient-specific induced pluripotent stem-cell models for long-QT syndrome. N Engl J Med. 2010; 363:1397–1409. [PubMed: 20660394]
48. Masumoto H, Matsuo T, Yamamizu K, Uosaki H, Narazaki G, Katayama S, et al. Pluripotent stem cell-engineered cell sheets reassembled with defined cardiovascular populations ameliorate reduction in infarct heart function through cardiomyocyte-mediated neovascularization. Stem Cells. 2012; 30:1196–1205. [PubMed: 22438013]

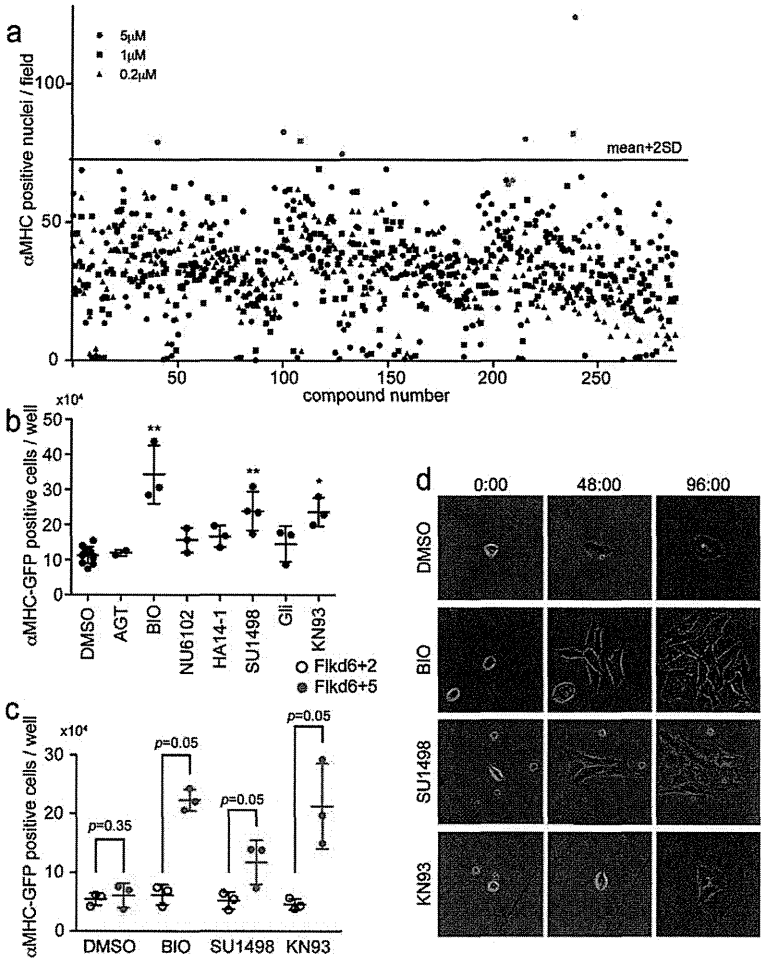

Figure 1.

Three Chemicals were Identified With Chemical Library Screening for mESCM Proliferation. (a) Primary screen with high content screening for nucleus numbers in αMHC-positive cells (mESCMs). Mean nucleus numbers at Flkd6+5 treated with approximately 280 chemicals at three concentrations (● 5μM, ■ 1μM, and ▲ 0.2μM, n = 2). Seven chemicals (red symbols) increased mESCMs more than mean + 2SD of control (control: n = 35). Two CaMKII inhibitors (blue symbols) increased mESCM more than mean + 1SD. (b) Secondary screen for the seven chemicals calculating actual cardiomyocyte numbers with flow cytometry. Abbreviation: Aminoglutethimide, AGT and Glibenclamide, Gli. Concentration: AGT 5μM, BIO 1μM, NU6102 5μM, HA14-1 1μM, SU1498 5μM, Gli 5μM and KN93 5μM. *, $p < 0.05$, **, $p < 0.01$ *vs.* DMSO treatment (Dunn's test for multiple comparisons, n = 3–11). (c) Chemicals increased mESCM numbers during Flkd6+2 to Flkd6+5. p value: Mann-Whitney test, n = 3. (d) Captured images from time-lapse video recording during Flkd6+0.5 (0:00) to 4.5 (96:00).

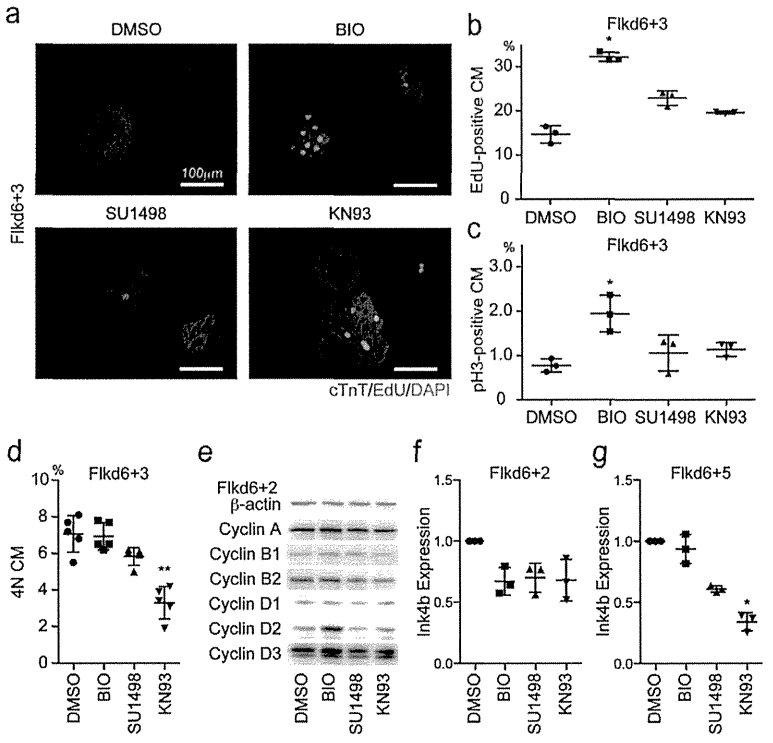

Figure 2.

Cell Cycle in mESCM was Enhanced by Identified Chemicals. (a) Immunostaining of purified mESCMs for cardiac troponin T (red), EdU (Green), and DAPI (Blue) at Flkd6+3. Scale bar = 100μm (b–c) Quantification of mESCMs positive for cell cycle markers (b) S phase (EdU-positive) and (c) M phase (phospho histone H3: pH3-positive) at Flkd6+3. *, $p < 0.05$ vs. DMSO group (Dunn's test, $n = 3$). (d) Quantification of 4N (Binuclear (2×2N) and G2/M) mESCMs by flow cytometry. **, $p < 0.01$ vs. DMSO group (Dunn's test, $n = 5$). (e) Western blotting for cyclins at Flkd6+2. BIO treatment increased Cyclin Ds. (f–g) qRT-PCR for *Ink4b*, a CDK inhibitor at Flkd6+2 (f) and Flkd6+5 (g). The expression of Ink4b was suppressed by all three chemicals at Flkd6+2 and more than 60% by KN93 at Flkd6+5. Relative expression levels compared to DMSO treatment group were shown. *, $p < 0.05$ and **, $p < 0.01$ vs. DMSO group (Dunn's test, $n = 3$).

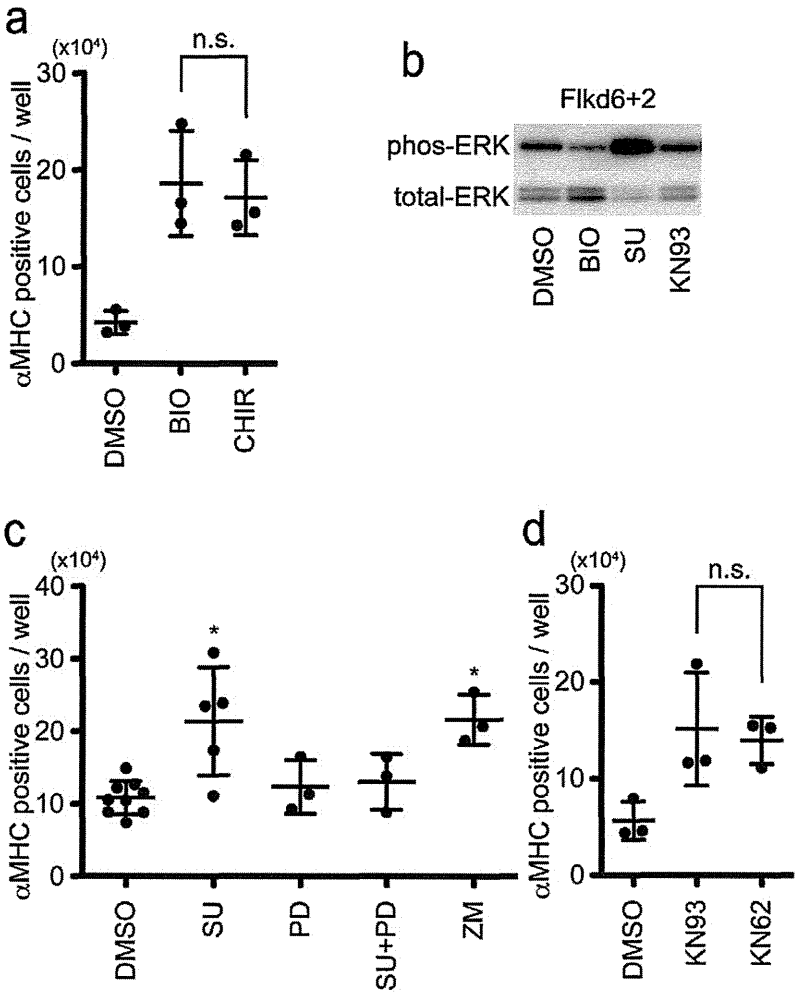

Figure 3.

Identified Chemicals were GSK3 Inhibitor, ERK Activator and CaMKII Inhibitor. (a) Effects of GSK3 inhibitors, BIO and CHIR99021 (CHIR) (Mann-Whitney test, $n = 3$) on mESCM numbers. (b) Western blotting for Phosphorylated ERK (phos-ERK) and total ERK at Flkd6+2. SU1498 treatment increased phos-ERK. (c) mESCM cell number at Flkd6+5. SU1498 (SU)-elicited mESCM proliferation was attenuated by a MEK inhibitor (PD98059, PD) treatment. A Raf activator (ZM336372, ZM) treatment also increased mESCM number. *, $p < 0.05$ *vs.* control group (Dunn's test, n = 3–9). (d) Effects of CaMKII inhibitors, KN93 and KN62, on mESCM numbers at Flkd6+5 (Mann-Whitney test, $n = 3$).

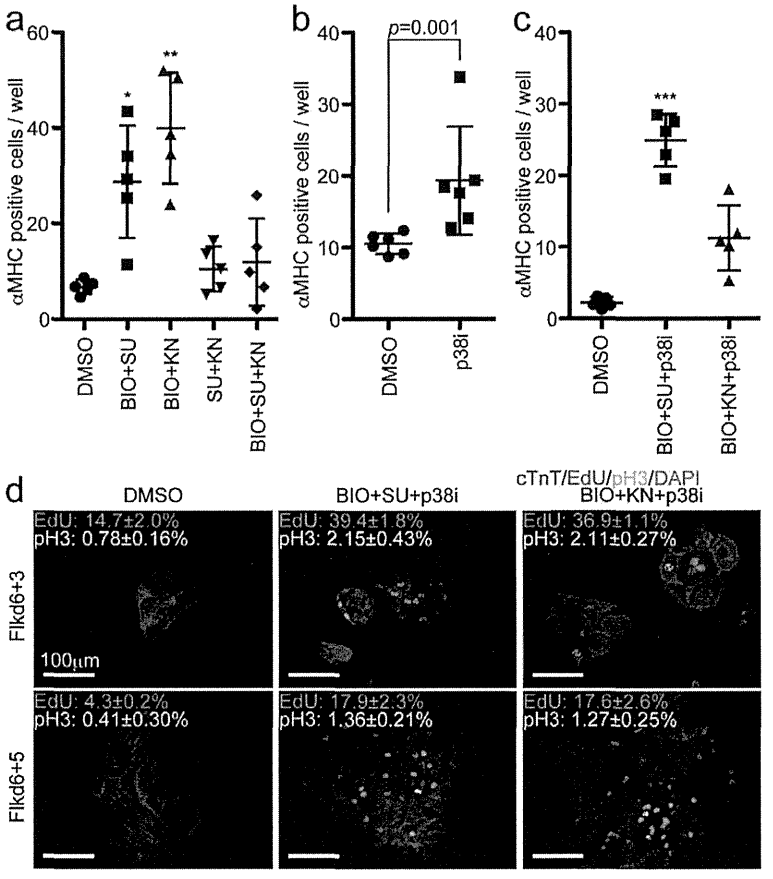

Figure 4.

Combination of Chemicals Synergistically Enhanced mESCM Proliferation. (a) Combinatory effects of chemicals on mESCM cell number (Dunn's test: *, $p < 0.05$ and **, $p < 0.01$, *vs.* DMSO treated group, n = 5) (b) Effects of a p38 inhibitor (p38i, SB203580). p value: Mann-Whitney test (n = 6) (c) Combinatory effects of chemicals on mESCM cell number in low cell density culture (Dunn's test: ***, $p < 0.001$, $n = 5$, *vs.* DMSO control). Note that BIO+SU+p38i treatment increased mESCM number 14-fold compared to DMSO treatment. (d) Immunostaining and quantification of cell cycle markers. Cardiac troponin T (cTnT, red), EdU (Green), phospho-histone H3 (pH3: white), and DAPI (Blue). Scale bar = 100 μm.

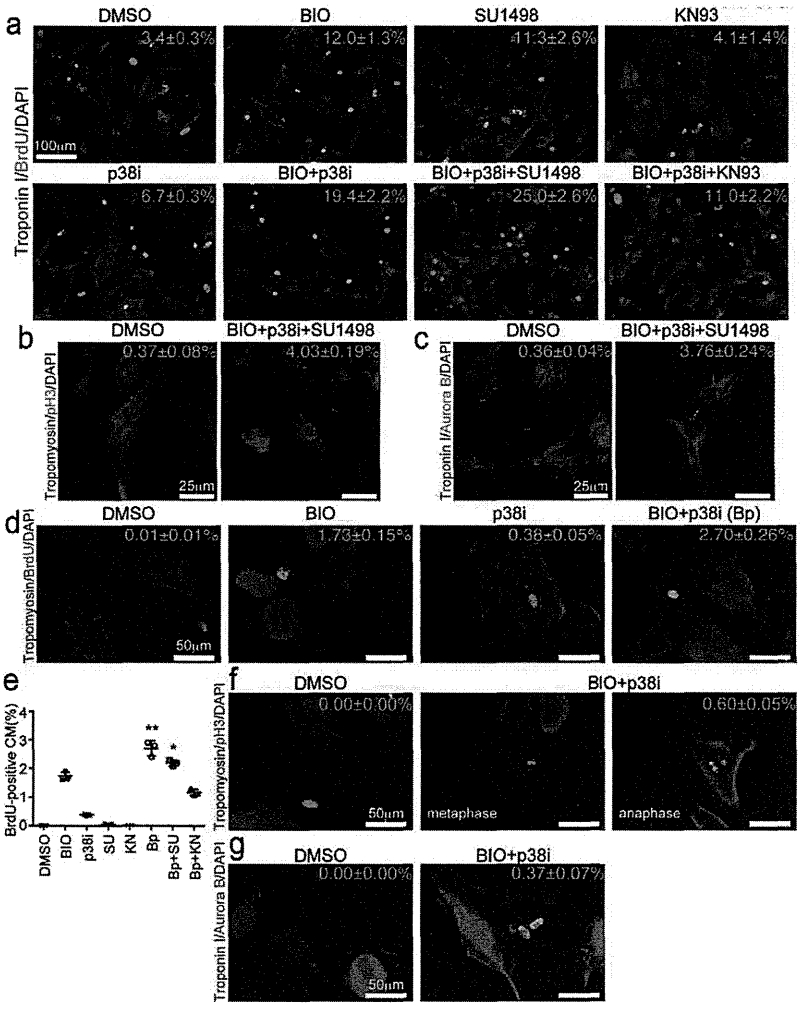

Figure 5.

Identified Chemicals Induced Cardiomyocytes Proliferation with Developmental Stage Specific Manner. (a–c) Immunostaining of neonatal rat cardiomyocytes for cell cycle analysis at day 2 after chemical treatment. (a) Troponin I (red), BrdU (green) and DAPI (blue). Scale bar = 100 μm (b) Tropomyosin (red), pH3 (green) and DAPI (blue). Scale bar = 25 μm (c) Troponin I (red), Arurora B (green) and DAPI (blue). Scale bar = 25 μm (d–g) Immunostaining of adult rat cardiomyocytes for cell cycle markers at day 6 after chemical treatment. (d) Tropomyosin (red), BrdU (green) and DAPI (blue). (e) Quantification of BrdU-positive cardiomyocytes. (Dunn's test: *, $p < 0.05$ and **, $p < 0.01$, *vs.* DMSO treated group, n = 3.) (f) Tropomyosin (red), pH3 (green) and DAPI (blue). (g) Troponin I (red), Aurora B (green) and DAPI (blue).

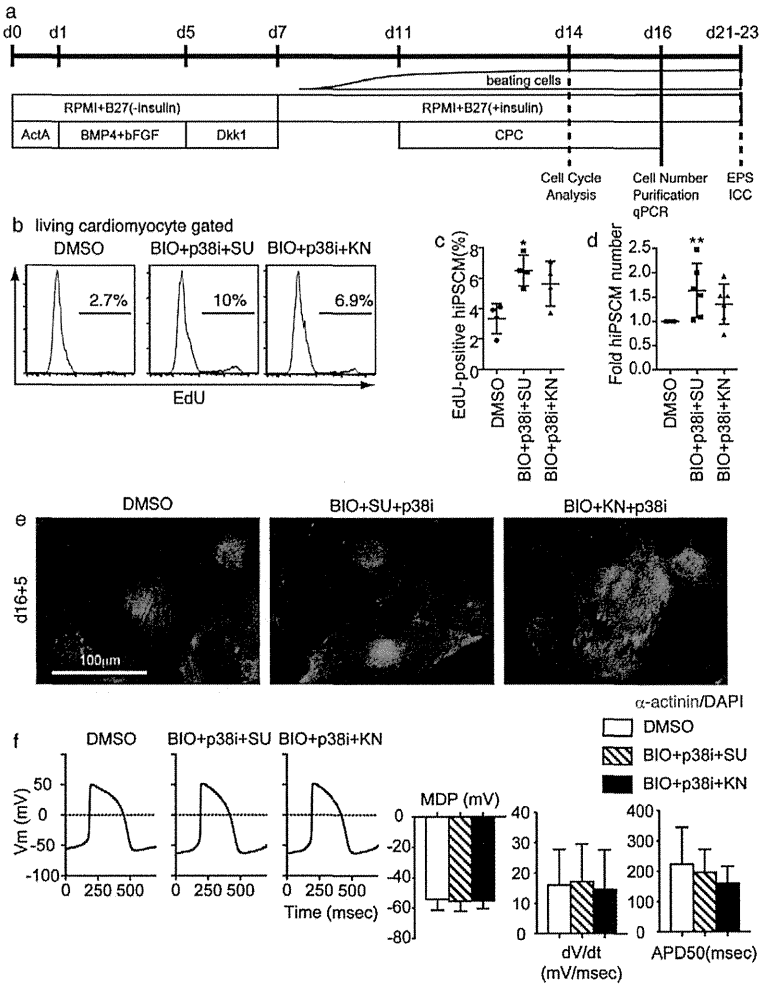

Figure 6.

Effects of Chemicals on Human iPSCs-Derived Cardiomyocytes. (a) Differentiation and experimental scheme for human iPSC study. Differentiation of human iPSCs was induced for 11 days. Cells were then treated by CPCs. (b) Representative plot of EdU in cardiomyocytes at d14. (c) EdU-positive ratio in cTnT-positive cell at d14 after induction. Dunn's test: *, $p < 0.05$, *vs.* DMSO treated group, n = 3.) (d) cTnT-positive cell number at d16. Dunn's test: *, $p < 0.05$, *vs.* DMSO treated group, n = 6.) (e) Immunostaining for α-actinin at d16+5-7. Scale bar = 100μm. (f) Representative action potential of purified VCAM1-positive cells and graphs for action potential parameters at d16+5. MDP, mean diastolic potential. dV/dt, maximum rate of depolarization. APD50, action potential duration. (i) Immuno staining for α-actinin at d16+5-7. No significant difference *vs.* control (n = 17).

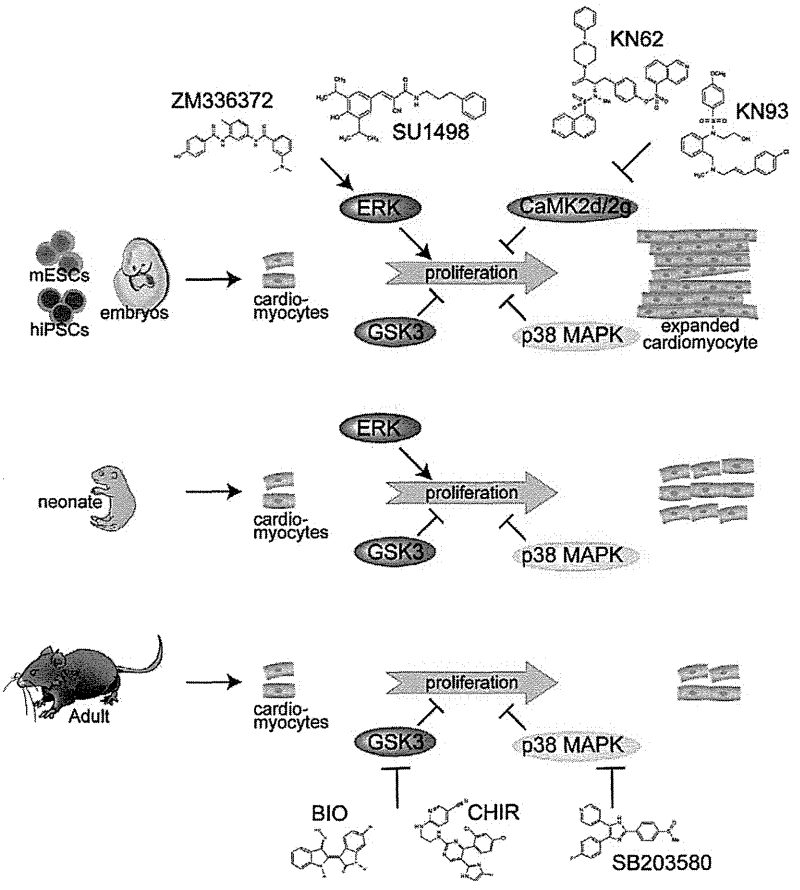

Figure 7.

Scheme of Regulatory Machinery of Cardiomyocyte Proliferation. Four distinct signaling pathways, GSK3, p38 MAPK, and CaMKII signaling negatively, and ERK signaling positively, regulate cardiomyocyte proliferation. Inhibitors for GSK3 (BIO and CHIR), p38 MAPK (SB203580), and CaMKII (KN93 and KN62), and activators for ERK (SU1498 and ZM336372) can be used to induce cardiomyocyte proliferation. A combinatory regulation of these signaling efficiently enhances each effect. We named these chemicals as cardiomyocyte proliferating chemicals (CPCs). CPCs show developmental stage-specific effects. CaMKII inhibitors act only on embryonic and PSC-derived cardiomyocytes. ERK activators still work on neonatal cardiomyocytes but not in adult cardiomyocytes. GSK3 and p38 MAPK inhibitors synergistically enhance cardiomyocyte proliferation broadly even in adults.

BJP British Journal of Pharmacology

DOI:10.1111/bph.12328
www.brjpharmacol.org

RESEARCH PAPER

Angiotensin II type 1a receptor signalling directly contributes to the increased arrhythmogenicity in cardiac hypertrophy

Shinji Yasuno[1,2], Koichiro Kuwahara[1], Hideyuki Kinoshita[1], Chinatsu Yamada[1], Yasuaki Nakagawa[1], Satoru Usami[1], Yoshihiro Kuwabara[1], Kenji Ueshima[2], Masaki Harada[1], Toshio Nishikimi[1] and Kazuwa Nakao[1]

[1]*Department of Medicine and Clinical Science, Kyoto University Graduate School of Medicine, Kyoto, Japan, and* [2]*EBM Research Center, Kyoto University Graduate School of Medicine, Kyoto, Japan*

Correspondence
Koichiro Kuwahara, Department of Medicine and Clinical Science, Kyoto University Graduate School of Medicine, 54 Shogoin Kawaharacho, Sakyo-ku, Kyoto 606-8507, Japan. E-mail: kuwa@kuhp.kyoto-u.ac.jp

All these authors take responsibility for all aspects of the reliability and freedom from bias of the data presented and their discussed interpretation.

Keywords
angiotensin; arrhythmia; hypertrophy; connexin

Received
3 December 2012
Revised
11 July 2013
Accepted
21 July 2013

BACKGROUND AND PURPOSE

Angiotensin II has been implicated in the development of various cardiovascular ailments, including cardiac hypertrophy and heart failure. The fact that inhibiting its signalling reduced the incidences of both sudden cardiac death and heart failure in several large-scale clinical trials suggests that angiotensin II is involved in increased cardiac arrhythmogenicity during the development of heart failure. However, because angiotensin II also promotes structural remodelling, including cardiomyocyte hypertrophy and cardiac fibrosis, it has been difficult to assess its direct contribution to cardiac arrhythmogenicity independently of the structural effects.

EXPERIMENTAL APPROACH

We induced cardiac hypertrophy in wild-type (WT) and angiotensin II type 1a receptor knockout (AT1aR-KO) mice by transverse aortic constriction (TAC). The susceptibility to ventricular tachycardia (VT) assessed in an *in vivo* electrophysiological study was compared in the two genotypes. The effect of acute pharmacological blockade of AT1R on the incidences of arrhythmias was also assessed.

KEY RESULTS

As described previously, WT and AT1aR-KO mice with TAC developed cardiac hypertrophy to the same degree, but the incidence of VT was much lower in the latter. Moreover, although TAC induced an increase in tyrosine phosphorylation of connexin 43, a critical component of gap junctional channels, and a reduction in ventricular levels of connexin 43 protein in both genotypes, the effect was significantly ameliorated in AT1aR-KO mice. Acute pharmacological blockade of AT1R also reduced the incidence of arrhythmias.

CONCLUSIONS AND IMPLICATIONS

Our findings demonstrate that AT1aR-mediated signalling makes a direct contribution to the increase in arrhythmogenicity in hypertrophied hearts independently of structural remodelling.

Abbreviations

WT, wild-type; AT1aR, angiotensin II type 1a receptor; AT1aR-KO, angiotensin II type 1a receptor knockout; TAC, transverse aortic constriction; LV, left ventricular; LVDd, left ventricular end-diastolic dimension; LVPW, left ventricular posterior wall; %FS, percent fractional shortening; RV, right ventricle; Cx43, connexin43; AT2R, angiotensin type 2 receptor; VT, ventricular tachycardia

Introduction

Heart failure is a leading cause of mortality and morbidity in the Western world (McKinsey and Olson, 2005). Despite the recent progress in both medical and non-medical treatment, the prognosis for patients with heart failure remains poor, with a 5-year survival rate of only about 50% (Zannad *et al.*, 1999; Levy *et al.*, 2002). Furthermore, up to 50% of the deaths among heart failure patients are sudden and unexpected, and are presumed to be the result of lethal arrhythmias (Tomaselli and Marban, 1999). For that reason, a fuller understanding of the molecular mechanisms underlying the increased arrhythmogenicity seen in failing hearts would be highly desirable.

Heart failure is often preceded by pathological enlargement of the heart due to cardiac muscle cell hypertrophy (Frey and Olson, 2003). Indeed, cardiac hypertrophy is a major risk factor for heart failure (Lauer *et al.*, 1999; Kannel, 2000; Vakili *et al.*, 2001; Devereux *et al.*, 2004; Gardin and Lauer, 2004; Okin *et al.*, 2004) and is also a risk factor for ventricular arrhythmias and sudden cardiac death (Levy *et al.*, 1987; Haider *et al.*, 1998). This suggests that there are shared pathways linking cardiac hypertrophy, heart failure and arrhythmias. Recent data showing a close association between ventricular hypertrophy and increased susceptibility to arrhythmia in a genetically engineered mouse model of hypertrophic cardiomyopathy support this notion (Wolf *et al.*, 2005). This increased susceptibility to arrhythmia reflects electrical remodelling that includes changes in the function and expression of membrane ion channels, gap junction proteins and Ca^{2+}-cycling proteins, and structural remodelling that includes alterations in composition of the extracellular matrix, that predisposes the hypertrophied ventricle to arrhythmogenic events such as early and delayed afterdepolarization and re-entry (Tomaselli and Marban, 1999).

Angiotensin II has been implicated in the development and progression of various cardiovascular diseases, including cardiac hypertrophy and heart failure. A number of large-scale randomized clinical trials have shown that reducing angiotensin II signalling by inhibiting ACE or blocking angiotensin type 1 receptor improves the prognosis and reduces disease severity in patients with heart failure (Howard *et al.*, 2006). Inhibiting angiotensin II signalling also reportedly reduces the incidences of both heart failure and sudden cardiac death (Kober *et al.*, 1995; Cleland *et al.*, 1997). Moreover, several studies of genetically modified animal models have clearly demonstrated the arrhythmic potential of angiotensin II signalling (Xiao *et al.*, 2004; Domenighetti *et al.*, 2007; Fischer *et al.*, 2007). However, because angiotensin II signalling also plays an important role in the structural remodelling (e.g. cardiomyocyte hypertrophy and cardiac fibrosis) seen during the development and progression of cardiac hypertrophy or cardiomyopathy, it has been difficult to obtain clear evidence of a direct contribution by angiotensin II signalling to the increase in arrhythmogenicity independently of structural remodelling.

Our aim in the present study was therefore to clarify the direct contribution of angiotensin II type1a receptor (AT1aR)-mediated signalling to the increase in arrhythmogenicity seen during cardiac remodelling. To accomplish this, we first induced cardiac hypertrophy in wild-type (WT) and angiotensin II type 1a receptor knockout (AT1aR-KO) mice by subjecting their hearts to chronic pressure overload caused by transverse aortic constriction (TAC) (Harada *et al.*, 1998b). We then carried out an *in vivo* electrophysiological study to compare arrhythmogenicity in the two genotypes. We also assessed the inhibitory effect of acute pharmacological blockade of AT1R on inducible arrhythmias in mice with TAC and the molecular mechanism by which AT1aR-mediated signalling makes a direct contribution to the electrical remodelling. Our results demonstrate that AT1aR-mediated signalling can make a direct contribution to the increase in arrhythmogenicity in hypertrophied hearts independently of structural remodelling.

Methods

Animal preparations

The animal care and all experimental protocols were reviewed and approved by the Animal Research Committee at the Kyoto University Graduate School of Medicine. AT1aR-KO ($AT1aR^{-/-}$) mice (C57BL/6 background) were kindly provided by Dr Fukamizu (The University of Tsukuba) (Sugaya *et al.*, 1995). WT C57BL/6 littermates served as controls.

Transverse aortic constriction

Eight- to ten-week-old mice were anaesthetized, intubated and artificially ventilated as previously described (Izumi *et al.*, 2001). Pressure overload was then induced by TAC (Hill *et al.*, 2000; Nakagawa *et al.*, 2006). Briefly, the chest cavity was opened in the second intercostal space, at the left sternal border, to expose the aortic arch. The segment of aortic arch between the right innominate and left carotid arteries was then constricted using a 7-0 silk suture tied firmly against a 27-gauge needle. The needle was subsequently removed, leaded to approximately 70% constriction. Sham-operated mice underwent the identical surgical procedure, except the aortic arch was not constricted. Four weeks after the sham or TAC operation, mice were killed by cervical dislocation and excised hears were used for further analyses.

Echocardiography

Echocardiography was carried out before (baseline) and 4 weeks after surgery using an echocardiographic system (Toshiba Power Vision 8000) equipped with a 12 MHz imaging transducer as described previously (Adachi *et al.*, 2003). Mice were anaesthetized with spontaneous respiration by i.p. injection of tribromoethanol/amylene hydrate (avertin) 2.5% w/v solution (8 $L \cdot g^{-1}$). We measured left ventricular (LV) end-diastolic dimension (LVDd), LV posterior wall (LVPW) thickness and percent fractional shortening (%FS).

Histological examination

Hearts were fixed in 10% formalin and prepared for histological analysis as described previously (Li *et al.*, 2002). To quantitate the myocardial fibrosis, we determined the ratios of the Sirius red-stained area to the total area. The data were then shown as % fibrosis, as previously reported (Li *et al.*, 2002).

Quantitative RT-PCR analysis

Using 50 ng of total RNA prepared from ventricles, levels of mouse *ANP*, *BNP*, *Acta1*, *SERCA2*, *TGF-β1*, *collagen 1*, *fibronec-*

tin, *CTGF*, *SCN5A*, *CACNA1c*, *KCND2*, *Kchip2*, *KCNJ2*, *KCNH2*, *KCNJ11* and *GAPDH* mRNA were determined using quantitative real-time PCR according to the manufacture's protocol (Applied Biosystems, Zaventam, Belgium). The sequences of the forward (F) and reverse (R) primers and of the probes (P) with fluorescent dye (FAM) and quencher (TAMRA) for *ANP*, *BNP*, *Acta1*, *SERCA2*, *TGF-β1* and *collagen 1* were reported previously (Li *et al.*, 2002; Kuwahara *et al.*, 2003). The primers and probes for *fibronectin*, *CTGF*, *SCN5A*, *CACNA1c*, *KCND2*, *Kchip2*, *KCNJ2*, *KCNH2*, *KCNJ11* and *GAPDH* were purchased from Applied Biosystems.

Intracardiac electrophysiology

The mice underwent intracardiac electrophysiological examination 4 weeks after TAC or sham operation. They were initially anaesthetized with ether and placed on a warm pad maintained at 37°C. The trachea of each mouse was then cannulated with a polyethylene tube, and the mice were respirated using a rodent respirator (Shinano Co., Tokyo, Japan) with the tidal volume set at 0.9 mL and the respiration rate set at 110 min^{-1}. The mice were anaesthetized with 0.5–1.5% isoflurane for the remainder of the surgical procedure. A surface frontal plane 6-lead ECG was obtained using clips placed on each limb, and a midline cervical incision was made to expose the right jugular vein. Using a jugular vein cutdown approach, a catheter (2.0F octapolar catheter with inter-electrode spacing of 0.5 mm, CIBer mouse EP; NuMed, Hopkinton, NY, USA) was blindly placed into the right ventricle (RV). We confirmed the proper positioning of the catheter at the end of the experiment. A standard electrophysiology protocol was performed as described previously (Gehrmann and Berul, 2000; Kuwahara *et al.*, 2003). Rapid RV pacing using the extra stimulation (S_1S_2) technique with 1–3 extra stimuli was performed to determine the RV refractory period and to attempt induction of ventricular arrhythmias: 10 pacing stimuli (S1; a coupling interval is 80–90 ms) followed by 2–3 extra stimulations (S2-4) were used to induce VT in experiments to see effects of TAC on WT and AT1aR-KO, and 10 pacing stimuli (S1; a coupling interval is 80 ms) followed by 2 extra stimulations (S2, S3) were used to induce VT in experiments to see effects of EXP-3174. Between these two slightly different protocols, VT induction rates in WT mice subjected to TAC were not significantly different (Tables 1 and 2). Note that the similar protocol is commonly used in electrophysiological studies with humans. The stimulation was applied at twice the ventricular diastolic capture threshold. VT was defined as an induction of three or more consecutive premature ventricular contractions. The operator who performed electrophysiological study was blinded to the genotype and procedure status of the experimental animals. In some experiments, 0.3 $mg \cdot kg^{-1}$ EXP-3174, an AT1R-blocking losartan metabolite, or vehicle was i.v. administered 60 min before the examination. We used EXP-3174 because it is the active carboxylic acid metabolite of losartan, exerts prompt pharmacological action, and has more potent and selective AT1R blocking activity than losartan (Chang *et al.*, 1995).

Immunoprecipitation and Western analyses

Details of the methods used to prepare lysates from the ventricles of sham- and TAC-operated mice, as well as those used to carry out co-immunoprecipitation assays, were described previously (Nakagawa *et al.*, 2006). Briefly, frozen samples of the ventricle were homogenized and sonicated in lysis buffer containing 20 mM Tris–HCl (pH 7.5), 150 mM NaCl, 1 mM Na_2EDTA, 1 mM EGTA, 1% Triton, 2.5 mM sodium pyrophosphate, 1 mM β-glycerophosphate, 1 mM Na_3VO_4, 1 $\mu g \cdot mL^{-1}$ leupeptin and 1 mM phenylmethylsulfonyl fluoride (Cell Signaling Technology, Inc., Danvers, MA, USA). After the debris was cleared by centrifugation, the protein concentration in the supernatant was quantified as the crude extract. For immunoprecipitation, 1 mg of extract was mixed with anti-connexin43 (Cx43) antibodies (1:50 dilution; Santa Cruz Biotechnology, Dallas, TX, USA) and protein A/G-PLUS-agarose (Santa Cruz) and then incubated overnight at 4°C.

Table 1

VT inducibility in WT and AT1aR-KO mice subjected to TAC or sham operation

	Total number of VT(+) mice	Induction rate of VT
WT-Sham ($n = 15$)	0	0%
KO-Sham ($n = 13$)	0	0%
WT-TAC ($n = 15$)	11	73.3%
KO-TAC ($n = 13$)	4	30.8%*

VT, ventricular tachyarrhythmia; WT-Sham, wild-type mice subjected to sham operation; KO-Sham, AT1aR-KO mice subjected to sham operation; WT-TAC, wild-type mice subjected to TAC; KO-TAC, AT1aR-KO mice subjected to TAC.
*$P < 0.05$ versus WT-TAC.

Table 2

Heart weight-to-body weight ratio, lung weight-to-body weight ratio and VT inducibility in WT mice subjected to TAC for 4 weeks then treated with either vehicle or EXP-3174

	Vehicle	EXP-3174
Body weight (g)	27.7 ± 0.1	27.4 ± 0.2
Heart weight (mg)	211.1 ± 5.6	213.4 ± 6.7
Lung weight (mg)	226.1 ± 3.9	241.9 ± 3.9
HW/BW ($mg \cdot g^{-1}$)	7.62 ± 0.23	7.82 ± 0.26
LW/BW ($mg \cdot g^{-1}$)	8.18 ± 1.43	8.87 ± 1.43
Total number of VT (+) mice	8	3
Induction rate of VT (%)	73	25*

HW/BW, heart weight-to-body weight ratio; LW/BW, lung weight-to-body weight ratio; vehicle, WT mice treated acutely with vehicle 4 weeks after TAC; EXP-3174, WT mice treated acutely with EXP-3174 4 weeks after TAC; VT, ventricular tachyarrhythmia; TAC, transverse aortic constriction. EXP-3174 (0.3 $mg \cdot kg^{-1}$) was given intravenously 1 h prior to the EPS study. $n = 11$ in the vehicle group and 12 in the EXP-3174 group.
*$P < 0.05$ versus control vehicle.

Precipitated proteins were separated by SDS-PAGE using 10% polyacrylamide gels and then analysed by Western blotting using anti-phosphotyrosine (1:200; Santa Cruz) and anti-Cx43 (1:1000; Santa Cruz) as probes. In addition, extract containing 50 μg of protein was used for Western blotting with anti-Cx43 (1:1000; Santa Cruz) or anti-β-actin (1:1000; Sigma-Aldrich, St. Louis, MO, USA) antibody as Input to control for variation in levels of protein expression. In another experiment, extracts containing 50 μg of protein were separated by SDS-PAGE using 15% polyacrylamide gels and then analysed by Western blotting using anti-Tyr^{265}-phosphorylated Cx43 (1:1000; Santa Cruz), anti-Cx43 (1:1000; Santa Cruz) or anti-GAPDH (1:1000; Merck Millipore, Billerica, MA, USA) antibody.

Statistical Analysis

Data are presented as means ± SEM. We compared continuous variables using Student's *t*-test. Frequency analysis was performed using chi square test. ANOVA with post hoc Fisher's protected least significant difference test was used for comparison among groups. Values of $P < 0.05$ were considered significant.

Results

TAC induced comparable cardiac hypertrophy in AT1aR-KO and WT mice

An earlier report showed that, in response to chronic pressure overload created by abdominal aortic banding, AT1aR-KO mice developed cardiac hypertrophy just as WT mice did (Harada *et al.*, 1998b). With that in mind, we aimed to use these mice to examine the role of AT1aR in the electrical remodelling seen during cardiac hypertrophy induced by chronic pressure overload caused by TAC. Echocardiographic examination revealed that before TAC or the sham operation, there were no significant differences in LVDd, LVPW thickness or %FS among the four groups studied (Figure 1A–C). However, LVPW thickness was significantly higher in both AT1aR-KO and WT mice 4 weeks after TAC than before it (0.61 ± 0.01 mm → 0.82 ± 0.02 mm and 0.63 ± 0.01 mm → 0.86 ± 0.02 mm, respectively, $P < 0.01$). As previously reported, there was no difference between the heart weight-to-body weight ratios in AT1aR-KO and WT mice following either TAC or sham operation (AT1aR-KO with sham, 4.3 ± 0.05 mg·g^{-1}; AT1aR-KO with TAC, 5.7 ± 0.22 mg·g^{-1};

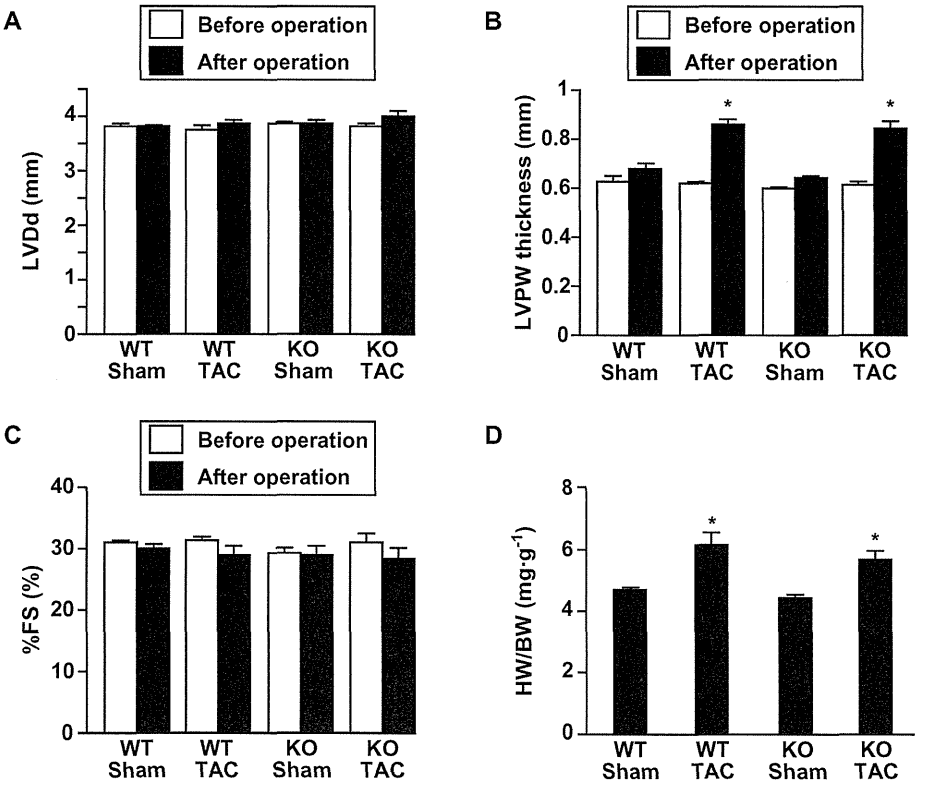

Figure 1

Angiotensin II type 1a receptor knockout (AT1a-KO) and wild-type (WT) mice develop left ventricular hypertrophy to a similar degree after transverse aortic constriction (TAC). Left ventricular (LV) end-diastolic dimension (LVDd) (A), left ventricular posterior wall (LVPW) thickness (B) and percent fractional shortening (%FS) (C) evaluated by echocardiography before and after TAC or sham operation. Values are means ± SEM. *$P < 0.01$ versus before each operation. (D) Heart weight-to-body weight (HW/BW) ratios 4 weeks after the operation. Values are means ± SEM. *$P < 0.01$ versus sham-operated mice in each genotype. WT-Sham, wild-type mice subjected to sham operation ($n = 37$); KO-Sham, AT1aR-KO mice subjected to sham operation ($n = 38$); WT-TAC, wild-type mice subjected to TAC ($n = 45$); KO-TAC, AT1aR-KO mice subjected to TAC ($n = 35$).

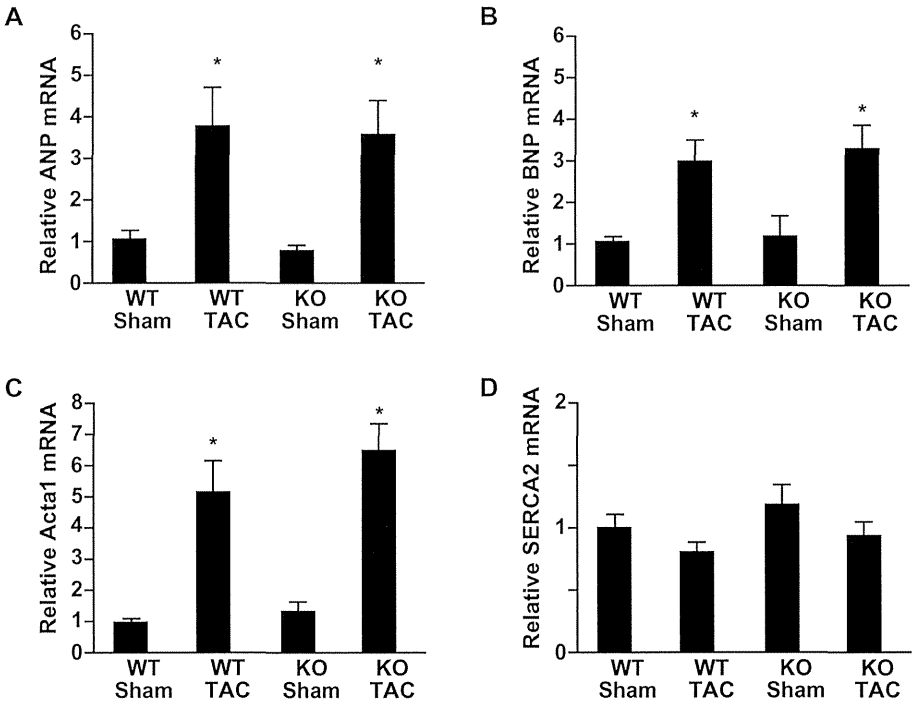

Figure 2

Effects of chronic pressure overload on left ventricular expression of hypertrophic marker genes 4 weeks after transverse aortic constriction (TAC) or sham operation. Relative expression levels of ANP (A), BNP (B), Acta1 (C) and SERCA2 (D) mRNA were normalized to the corresponding GAPDH mRNA levels. The mean relative level of each mRNA in sham-operated wild-type (WT) mice was assigned a value of 1.0. Values are means ± SEM (n = 8 each). *P < 0.01 versus sham-operated mice of each genotype.

WT with sham, 4.6 ± 0.06 mg·g^{-1}; WT with TAC, 6.1 ± 0.25 mg·g^{-1}) (Figure 1D). Likewise, expression of hypertrophic and fibrotic marker genes induced in response to the chronic pressure overload was quite similar in AT1aR-KO and WT mice (Figures 2A–D and 3A–D), and histological analysis showed that pressure overload induced similar degrees of cardiac fibrosis in AT1aR-KO and WT mice (Figure 3E and F), which is consistent with the notion that AT1aR-mediated signalling is dispensable for the structural remodelling induced by TAC. Angiotensin type 2 receptor (AT2R) expression did not significantly differ between AT1aR-KO and WT mice, with or without TAC, as reported previously (data not shown here) (Harada *et al.*, 1998b).

Diminished induction of ventricular tachycardia in AT1aR-KO mice

Given that AT1aR-KO mice and their WT littermates showed similar structural remodelling in response to chronic pressure overload, we next compared the electrical properties in the two genotypes. To accomplish this, 4 weeks after the sham operation or TAC, we inserted an octapolar 2.0F catheter into the RV via the right jugular vein and assessed the inducibility of ventricular tachycardia (VT) in the mice (Table 1). Figure 4A shows a representative polymorphic VT induced by programmed ventricular stimulation. There was no induction of VT in sham-operated AT1aR-KO or WT mice. Meanwhile, VT was induced in 11 of 15 (73.3%) WT mice subjected to TAC, but in only 4 of 13 (30.8%) AT1aR-KO mice with TAC. Thus, AT1aR deficiency had a significant (P < 0.05) protective effect against induction of VT in hypertrophied hearts.

Comparable ion channel gene expression in AT1aR-KO and WT mice

The ventricular expression of genes encoding ion channels has been shown to be altered during cardiac hypertrophy (Tomaselli and Marban, 1999). To test whether a difference in ion channel gene expression in the ventricular myocardium contributes to the difference in susceptibility to VT seen in AT1aR-KO and WT mice with TAC, we used real-time PCR to compare the transcription levels of several ion channel genes in the two genotypes, including those responsible for the I_{Na} (SCN5A), $I_{Ca\text{-}L}$ (CACNA1C), I_{TO} (KCND2 and Kchip2), I_{K1} (KCNJ2), I_{Kr} (KCNH2) and $I_{K\text{-}ATP}$ (KCNJ11). We found no significant difference in the levels of any of the corresponding mRNAs between AT1aR-KO and WT mice subjected to TAC or sham operation (Figure 4B).

Attenuated tyrosine phosphorylation and preserved levels of connexin 43 protein in AT1aR-KO ventricles

Gap junctions are clusters of intercellular channels that mediate electrical communication between adjacent cells. Connexin 43(Cx43) is the predominant ventricular gap junction protein, and under various conditions, it is phosphorylated at multiple serine residues by PKC and MAPK, and at

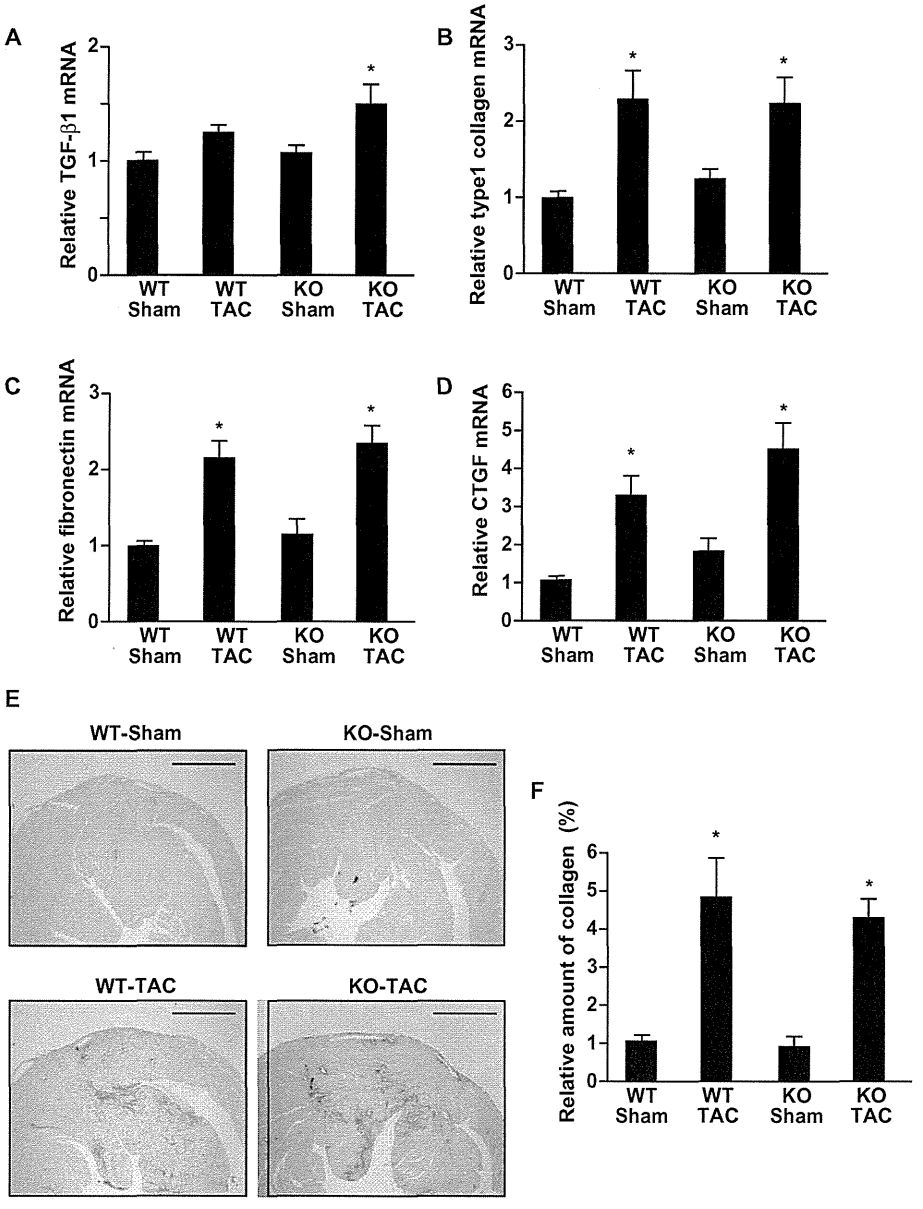

Figure 3

Effects of chronic pressure overload on cardiac fibrosis in wild-type (WT) and angiotensin II type 1a receptor knockout (AT1aR-KO) mice. (A–D) Left ventricular expression of fibrotic marker genes 4 weeks after transverse aortic constriction (TAC) or sham operation. Relative expression levels of TGF-β1 (A), type 1 collagen (B), fibronectin (C) and CTGF (D) mRNA were normalized to corresponding GAPDH mRNA levels. The mean relative level of each mRNA in sham-operated WT mice was assigned a value of 1.0. Values are means ± SEM ($n = 8$ each). *$P < 0.01$ versus sham-operated mice of each genotype. (E) Sirius red-stained sections of left ventricle from the both AT1aR-KO and WT mice processed 4 weeks after TAC or sham operation. Scale bars are 1 mm. (F) The relative fibrotic areas in left ventricles from AT1aR-KO and WT mice 4 weeks after TAC or sham operation. The mean value of the relative fibrotic area in left ventricles from sham-operated WT mice was assigned a value of 1.0. Values are means ± SEM ($n = 8$ each). *$P < 0.01$ versus sham-operated mice of each genotype.

two tyrosine residues by c-src (Lampe and Lau, 2004). Phosphorylation of Cx43 affects its tissue level, intracellular distribution and function (Toyofuku *et al.*, 2001; Warn-Cramer and Lau, 2004). The changes in gap junctions caused by Cx43 phosphorylation likely contribute to an overall reduction in conduction velocity and increased dispersion of action potential duration and refractory properties, which combine to form the substrate for potentially lethal arrhythmias (Gutstein *et al.*, 2001; Danik *et al.*, 2004; Poelzing and Rosenbaum, 2004; van Rijen *et al.*, 2004; King *et al.*, 2013). Indeed, a recent study showed the relationship between reduced conduction velocity and arrhythmogenicity in mouse hearts (King *et al.*, 2013). Mice with cardiac-restricted deletion of Cx43 showed slow conduction velocity in the heart, resulting in sudden arrhythmic death (Gutstein *et al.*, 2001). Furthermore, angiotensin II signalling reportedly